# Enrichment and Expansion with Nanoscale Artificial Antigen Presenting Cells for Adoptive Immunotherapy

Karlo Perica,[†,‡] Joan Glick Bieler,[⊥] Christian Schütz,[‡,⊥] Juan Carlos Varela,[‡,§] Jacqueline Douglass,[∥] Andrew Skora,[∥] Yen Ling Chiu,[‡,§] Mathias Oelke,[‡] Kenneth Kinzler,[∥] Shibin Zhou,[∥] Bert Vogelstein,[∥] and Jonathan P. Schneck*[,⊥,‡,†]

[†]Department of Biomedical Engineering, [‡]Institute of Cell Engineering, [§]Sidney Kimmel Comprehensive Cancer Center, [⊥]Department of Pathology, Johns Hopkins School of Medicine, Baltimore, Maryland 21205, United States and [∥]Ludwig Cancer Research Center and Howard Hughes Medical Institute, Johns Hopkins School of Medicine, Baltimore, Maryland 21205, United States

**ABSTRACT** Adoptive immunotherapy (AIT) can mediate durable regression of cancer, but widespread adoption of AIT is limited by the cost and complexity of generating tumor-specific T cells. Here we develop an Enrichment + Expansion strategy using paramagnetic, nanoscale artificial antigen presenting cells (aAPC) to rapidly expand tumor-specific T cells from rare naïve precursors and predicted neo-epitope responses. Nano-aAPC are capable of enriching rare tumor-specific T cells in a magnetic column and subsequently activating them to induce proliferation. Enrichment + Expansion resulted in greater than 1000-fold expansion of both mouse and human tumor-specific T cells in 1 week, with nano-aAPC based enrichment conferring a proliferation advantage during both *in vitro* culture and after adoptive transfer *in vivo*. Robust T cell responses were seen not only for shared tumor antigens, but also for computationally predicted neo-epitopes. Streamlining the rapid generation of large numbers of tumor-specific T cells in a cost-effective fashion through Enrichment + Expansion can be a powerful tool for immunotherapy.

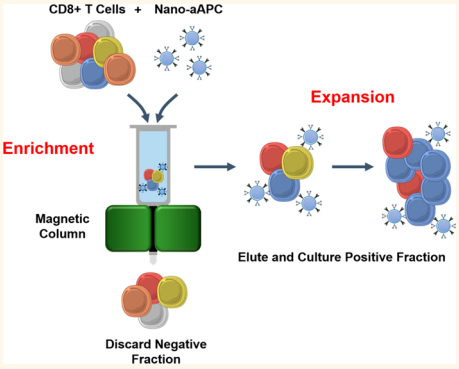


**KEYWORDS:** immunotherapy · nanoparticles · adoptive immunotherapy

Adoptive transfer of tumor-specific T cells can mediate durable regression of cancer.[1] While tumor-specific T cells can be derived from tumor infiltrating lymphocytes (TILs) or from cells engineered to express antitumor receptor transgenes,[2,3] cells derived from the endogenous naïve repertoire[4] possess several advantages. Unlike transgenic T cells, autologous naïve T cells have undergone central tolerance in the host, minimizing the risk of on-target autoimmunity.[5,6] Compared to TILs, endogenous naïve cells have not been activated in the exhaustive[7] and immunosuppressive[8] tumor microenvironment, and can be a source of tumor-specific cells even in patients who lack pre-existing antitumor responses.[9]

Tumor-specific cells from naïve precursors are generated by stimulation with tumor antigen presented on antigen-presenting cells (APC), complex biologics that are derived for each individual patient.[10] The additional culture process required to generate APC significantly increases the cost and complexity of adoptive immunotherapy. Furthermore, APC derived from cancer patients are often dysfunctional[11] or immunosuppressive,[12,13] further complicating the culture process.

We therefore designed an acellular T cell expansion platform termed nanoscale artificial Antigen Presenting Cells (nano-aAPC).[14] Nano-aAPC are paramagnetic iron-dextran nanoparticles, 50−100 nm in diameter, functionalized with major histocompatibility complex (MHC)-peptide to bind and activate antigen-specific TCR, and a costimulatory anti-CD28 antibody to promote effective T cell stimulation. We have previously demonstrated that nano-aAPC can induce robust expansion of human memory T cells and transgenic mouse cells.[14]

However, we and others have not been able to target the naïve T cell repertoire,

* Address correspondence to jschnec1@jhmi.edu.

Received for review January 13, 2015 and accepted July 1, 2015.

**Published online July 14, 2015**
**10.1021/acsnano.5b02829**

© 2015 American Chemical Society

which has a higher threshold for activation[15] than the memory pool. TCR are clustered at the nanoscale in a physiologically regulated fashion,[16] ultimately resulting in decreased binding of TCR on naïve cells by nanoparticles.[17] Despite this challenge, nanoparticles are preferred to microparticle based platforms because they are significantly more biocompatible and have favorable *in vivo* trafficking and biodistribution,[18−20] making them compatible for *in vivo* infusion. Furthermore, the first TCR signaling events occur in nanoscale TCR clusters,[17,21] suggesting that under appropriate conditions 50−100 nM nano-aAPC could be used to engage and activate robust TCR signaling.

Tumor-specific naïve precursors are extremely rare, with frequencies reported as few as one per million, more than an order of magnitude lower than the antiviral immune response.[22−24] APC-based methods for primary naïve tumor-specific cell expansion thus require stimulation over many weeks or months, often followed by T cell selection and subcloning,[25] to generate the large number of tumor specific cells required for adoptive immunotherapy.[26−28] The ideal T cell expansion platform would generate robust expansion that minimized culture time and reduced expense.

To meet these requirements, we hypothesized that enrichment of antigen-specific cells *prior* to activation and culture would reduce competition for growth signals such as cytokines and MHC binding. We therefore utilized nano-aAPC to bind and capture antigen-specific cells in a magnetic column prior to culture, the first use of a single platform to enrich and subsequently expand a targeted T cell population *in vitro*.

Here, we show that Enrichment + Expansion (E+E) streamlines the generation of large numbers and high frequencies of antigen-specific cells from naive precursors. Moreover, we find that enrichment prior to expansion confers a proliferation advantage during both *in vitro* culture and after *in vivo* adoptive transfer. This approach reliably expands T cells recognizing not only previously known "shared" tumor antigens, but also computationally predicted "neo-epitopes" based on unique tumor mutation patterns.[29] This is the first *in vitro* generation of antitumor responses against predicted neo-epitope responses from naïve cells, and could thus form the basis of a personalized tumor immunotherapy strategy even in patients who lack pre-existing responses.

## RESULTS AND DISCUSSION

**Antigen-Specific T Cell Enrichment with Nano-aAPC.** T cell stimulation requires two activating signals delivered by endogenous APC: signal 1, a cognate antigenic peptide presented in the context of MHC that binds the TCR; and signal 2, one of a number of costimulatory receptors that modulate T cell responses.[30] Nano-aAPC are synthesized by coupling chimeric MHC-Ig dimer (signal 1) and anti-CD28 antibody (signal 2) to 50−100 nm paramagnetic iron-dextran nanoparticles (Figure 1A).

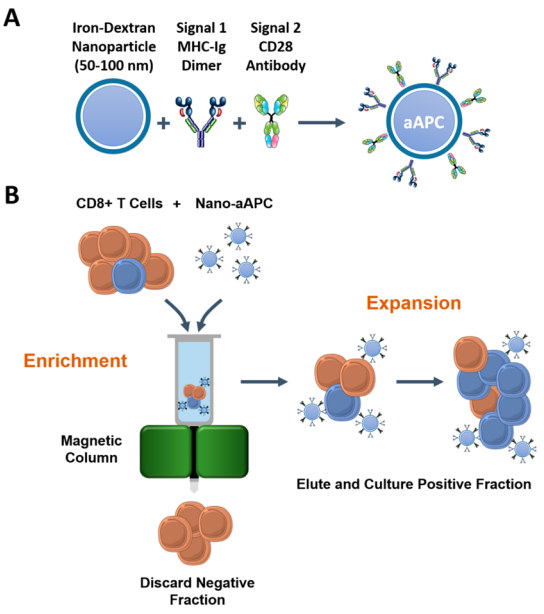


**Figure 1. Schematic of enrichment + expansion strategy. (A) Nanoscale artificial antigen presenting cells (nano-aAPC) are synthesized by coupling MHC-Ig dimer (Signal 1) and a costimulatory anti-CD28 antibody (Signal 2) to a 50−100 nm iron-dextran nanoparticle. (B) Schematic of magnetic enrichment. Antigen-specific CD8+ T cells (blue) bound to nano-aAPC are retained in a magnetic column in the "enrichment" step, while noncognate (orange) cells are less likely to bind. Enriched T cells are then activated by nano-aAPC and proliferate in the "expansion" step.**

Enrichment with nano-aAPC is performed by incubating naive, polyclonal mouse CD8+T lymphocytes with nano-aAPC, passing the cell-particle mixture through a magnetic column, eluting and then culturing the magnet-bound fraction (Figure 1B). To assess efficacy of enrichment prior to culture, a known number of Thy1.1+ pmel TCR transgenic T cells specific for Db-GP100 melanoma antigen were mixed at a 1:1000 ratio with Thy1.2+ CD8 T cells from wild type B6 mice. After enrichment with Db-GP100 aAPC, the frequency of pmel T cells increased more than 10-fold, from 0.07% before enrichment to 1.17% after enrichment, in a dose-dependent manner (Figure 2a). Optimizing the amount of nano-aAPC incubated with T cells increased the enrichment efficiency and resulted in recovery of up 95% of the added pmel T cells (Figure 2B).

Enrichment of wild-type Db-GP100 cells from endogenous B6 CD8+ splenocytes was assessed by staining with soluble MHC pentamer. Db-GP100 specific frequency was undetectable prior to enrichment, but increased to 0.30% afterward. The frequency of nonspecific Kb-TRP2 cells incubated with Db-GP100 particles did not increase (Figure 2C).

**Antigen-Specific T-Cell Expansion after Enrichment.** Enrichment + Expansion was performed using nano-aAPC bearing the melanoma antigens TRP2 (Kb-TRP2) and GP100 (Db-GP100), the Kb-restricted ovalbumin

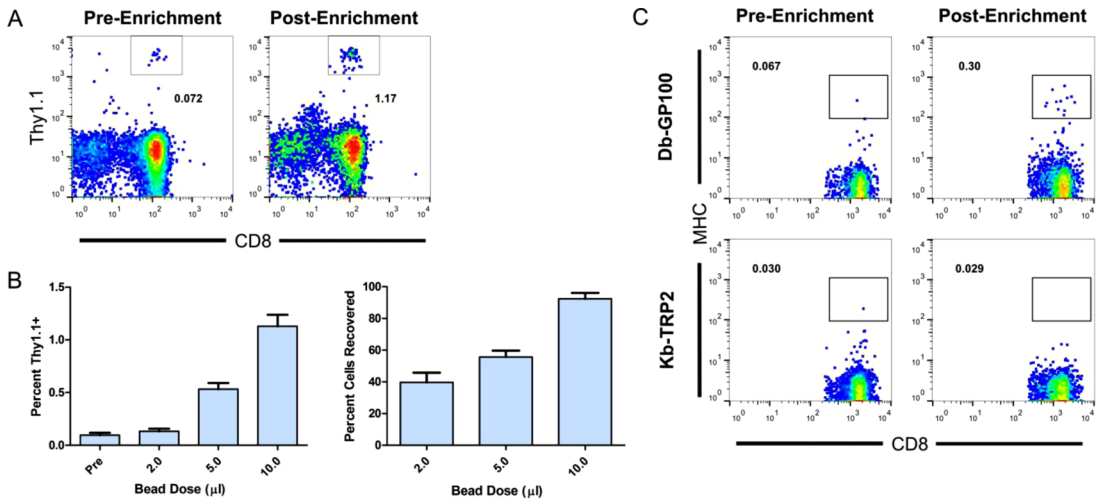


**Figure 2. Nano-aAPC mediated enrichment of antigen-specific T cells. (A) Nano-aAPC mediate antigen-specific enrichment of cognate, Thy1.1+ pmel cells from a pool of thousand-fold more polyclonal, Thy1.2+ B6 splenocytes. (B) Summary of antigen-specific cell frequency and percent cells recovered after pmel enrichment performed as in A with increasing amounts of nano-aAPC. Doses expressed as volume of an 8.3 nm solution. (C) Enrichment of endogenous Db-GP100 splenocytes by nano-aAPC (top). Frequency of noncognate Kb-TRP2 cells does not increase after enrichment (bottom).**

antigen SIIN (Kb-SIIN), and the colon carcinoma antigen Ld-AH1/A5 (Ld-A5); peptide sequences and proteins of origin are listed in Table S1. After enrichment, magnet-bound fractions of enriched cells and nano-aAPC were eluted and cultured *in vitro*. Seven days after enrichment, antigen-specific populations were detectable by MHC multimer staining for all four antigens examined (Figure 3A). Antigen-specific frequencies and absolute numbers of cells generated in 1 week varied by antigen. Kb-TRP2 and Kb-SIINF consistently generated a higher frequency of antigen specific cells (13.9 $\pm$ 5.2% and 20.0 $\pm$ 9.2%, respectively) than Db-GP100 or Ld-A5 (4.3 $\pm$ 0.6% and 6.9 $\pm$ 0.1%, respectively) (Figure 3B). This was reflected in the total number of antigen-specific cells that could be generated in 1 week from 10 million precursors, which ranged from 130 000 $\pm$ 10 000 for Kb-TRP2 to 35 000 $\pm$ 10 000 for Db-GP100 (Figure 3B; Table 1).

To study the effect of enrichment on subsequent proliferation, the enrichment procedure was "undone" in control samples by collecting the negative fraction (CD8+ T cells that passed through the magnetic column) and adding it back to the positive fraction (Figure 3C). Thus, we compared cells that had undergone the same nano-aAPC binding and culture process as E+E cells, but did not have the benefit of enrichment, to those that had been enriched. Enrichment significantly enhanced both antigen-specific frequency and total antigen-specific cell yield. In a representative sample, 7 days after enrichment with a Kb-TRP2 nano-aAPC, 17.6% of cells expanded from the positive fraction were Kb-TRP2 specific, compared to 1.46% of cells from the control unenriched group (Figure 3D). Similarly, 4.59% of Db-GP100 Positive fraction cells were antigen specific, compared to 0.45% in the unenriched group (Figure 3D). On average, E+E yielded a 12.2 $\pm$ 2.3 fold-increase in the frequency for Kb-TRP2, a 36.4 $\pm$ 14.9 fold increase for Db-GP100, and a 19.9 $\pm$ 11.6 fold increase for Kb-SIINF-specific T cells (Figure 3E). Enrichment also significantly increased the total number of antigen-specific cells, ranging from a 3.5 $\pm$ 0.4 fold increase for Kb-TRP2 to 7.6 $\pm$ 0.9 fold for Kb-SIINF and 11.1 $\pm$ 4.1 fold for Db-GP100 (Figure 3E; see Figure S1 for absolute antigen-specific frequency and total antigen-specific cells yields).

Effective enrichment was achieved with nano- but not microscale aAPC. Micro-aAPC made from 4.5 $\mu$m diameter iron-dextran particles and coated with MHC-Ig dimer and anti-CD28 were synthesized as described previously.[31] T cells frequently formed conjugates with noncognate micro-aAPC, resulting in little to no enrichment of antigen-specific cells (Figure S2). In contrast, nano-aAPC bound T cells with high specificity and low background. Thus, using our current formulations, nano-aAPC are a more effective reagent for antigen-specific enrichment.

**Fold-Expansion.** T cell proliferation was estimated from previously determined precursor frequencies (Table 1). Precursor frequencies for CD8 responses to foreign antigens range from 10 to 100 cells per 10 million T-cells.[24] Self-antigens such as TRP2 are expected to be at the lower end of this range. Precursor frequencies for Db-GP100 have been measured at 10 cells per $10^7$ T-cells,[22] and 20−350 cells per $10^7$ T-cells for Kb-SIINF.[24] After 1 week, 130 000 TRP2-specific cells were generated from $10^7$ CD8 T cells; thus, we estimate TRP2-specific proliferation was 1000- to 10 000-fold. In comparison, approximately 35 000 Db-GP100 and 150 000 Kb-SIINF specific T cells were generated from $10^7$ T cells, indicating up to 5000 fold expansion for each antigen. This is comparable to the robust expansion observed after viral infection *in vivo*.[32]

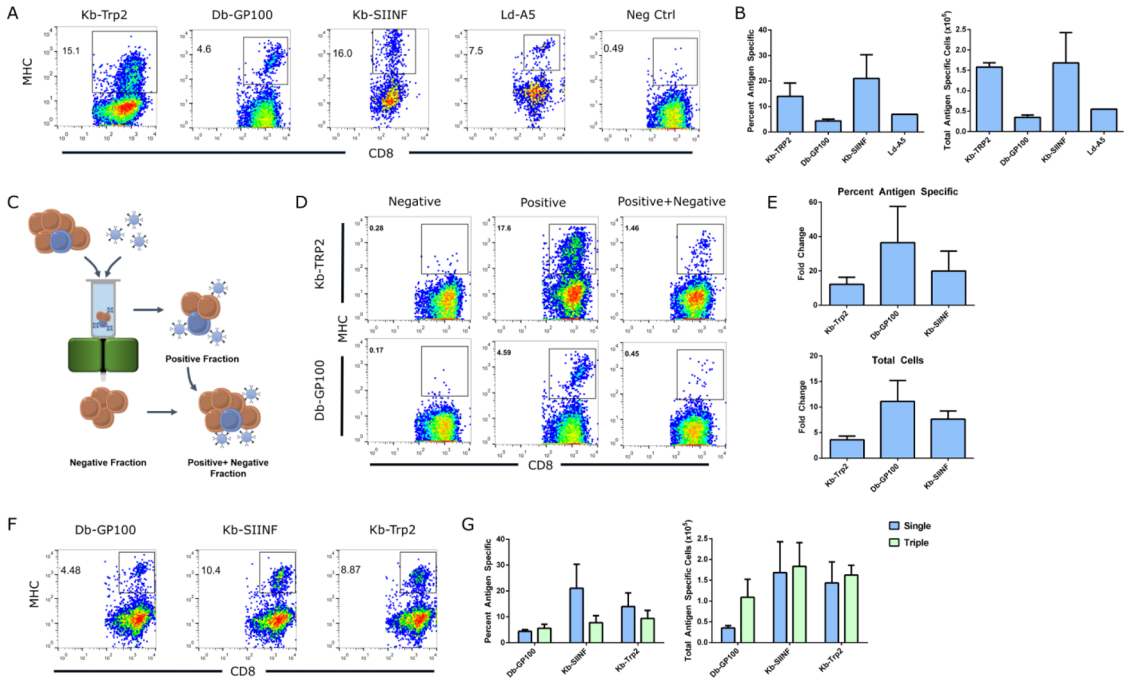


**Figure 3. Expansion of antigen-specific T cells after enrichment. (A) Representative FACS plots of Kb-TRP2, Db-GP100, Kb-SIINF, and Ld-A5 nano-aAPC expansion 7 days after enrichment with cognate nano-aAPC. (B) Summary of percent antigen-specific cells (left) and total antigen specific cells (right) after enrichment and expansion with indicated nano-aAPC after 7 days. Mean and standard deviation of three experiments. (C) Schematic of cell fractions used to assess effect of enrichment on expansion. Particle-bound antigen-specific T cells are captured in a magnetic column (positive fraction), whereas unbound cells pass through (negative fraction). The negative fraction can be added back to the positive fraction to undo the effect of enrichment (positive+negative). (D) Increased frequency of antigen-specific cells generated after 7 days of culture as a result of enrichment with nano-aAPC. Negative (left), positive (middle) and positive+negative (right) fractions were cultured for 7 days, then stained with cognate MHC dimer: either Kb-TRP2 (top) or Db-GP100 (bottom). (E) Fold increase in frequency (top) and total antigen-specific cell number (bottom) for cells enriched (positive) compared to not enriched (positive+negative) for the three antigens shown. (F) Three antigens (Db-GP100, Kb-SIINF, Kb-TRP2) enriched and expanded simultaneously. Representative FACS plots of antigen-specificity for each antigen from the same T cell culture. (G) Comparison of antigen-specificity (left) and total antigen-specific cells (right) generated for the three indicated antigens when enriched and expanded individually (Single, blue) or together (Triple, green).**

**TABLE 1. Antigen-Specific T Cell Expansion[a]**

| antigen | precursor frequency (per 10 million cells) | Ag-specific cells | fold expansion |
|---|---|---|---|
| Kb-TRP2 | 10−100[24] | 130 000 ± 80 000 | 1300−13 000× |
| Db-GP100 | 10−100[22] | 35 000 ± 10 000 | 350−3500× |
| Kb-SIINF | 20−350[24] | 150 000 ± 75 000 | 450−7500× |
| A2-NY-ESO1 | 36[55] | 44 000 ± 21 000 | 1200× |
| A2-MART1 | 1000[55] | 83 000 ± 37 000 | 83× |

[a] Estimated T cell precursor frequencies per 10 million lymphocytes (see references). Antigen-specific cells generated from 10 million lymphocytes.

To validate these estimates, we labeled naive T cell populations with the proliferation marker dye CFSE, which is diluted 2-fold with every round of T cell division. Four days following E+E, Kb-TRP2 tetramer binding T cells had diluted their CFSE below detectable limits (Figure S3a). Transgenic pmel T cells stimulated with a moderate dose of nano-aAPC were used for comparison; these cells showed multiple peaks of CFSE fluorescence, indicating between 2 and 7 rounds of division. By comparison, Enriched + Expanded TRP2-specific T cells had completed more than 7 rounds of division, consistent with greater than 256-fold expansion after only 4 days, in line with estimates of precursor frequency. Expanded T cells, both TRP-2 as well as SIY-specific, showed a CD62L-low, CD44-high effector memory phenotype (see Figure S3b for details), consistent with robust activation and proliferation.

T cell expansion by E+E was significantly more robust than expansion using mature, bone marrow derived dendritic cells pulsed with TRP2 peptide[33] (Figure S4a). Stimulation of ten million naive lymphocytes for 1 week resulted in $2 \pm 0.5 \times 10^4$ TRP2-specific T cells, with antigen-specific frequencies between 0.5−2.85%, approximately 10-fold lower in number and frequency than that achieved with E+E (Figure S4b). This is consistent with expansion by APC and artificial APC in humans, where antigen-specific responses after 1 week of stimulation are frequently not detectable.[34]

**Simultaneous Expansion of Multiple Antitumor Responses.** Simultaneous generation of T cell responses to multiple tumor antigens would increase the number of antitumor T cells generated from a single naive T cell population, and reduce the likelihood of tumor immune escape due to down-regulation of a single

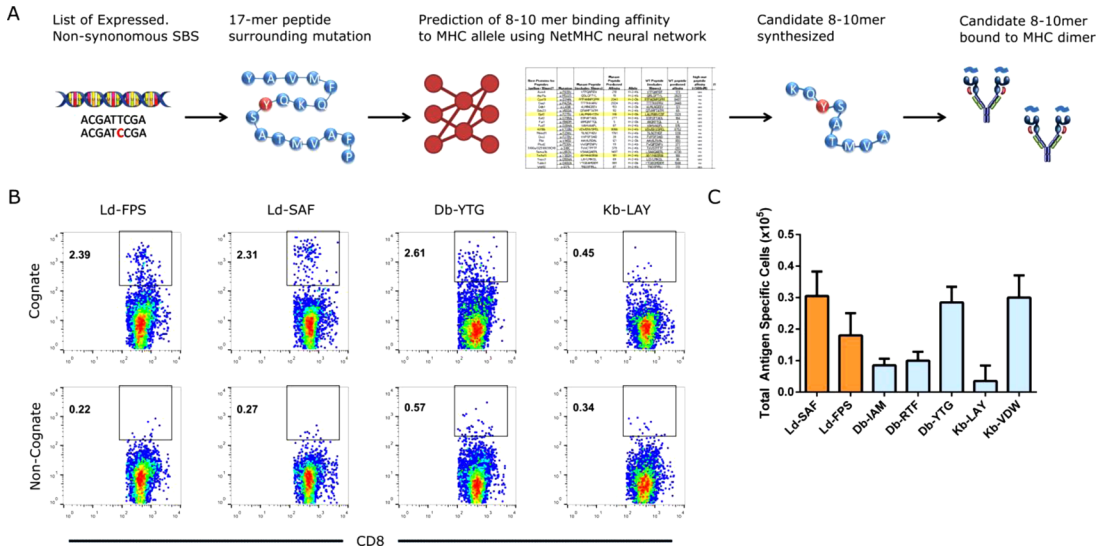


**Figure 4. Neo-epitope expansion. (A) Schematic of process for generating candidate peptides for B16 and CT26 mutomes. 17-mer sequences surrounding single-base pair substitutions (SBS) are assessed for MHC binding by MHCNet prediction algorithm. (B) Representative binding of cells expanded with nano-aAPC E+E for 7 days against neo-epitopes to cognate (top) and noncognate (bottom) MHC. (C) Total neo-epitope specific cells obtained at 1 week after E+E.**

antigen.[35−37] We therefore developed a single-step E+E protocol for generating multiple antitumor populations simultaneously.

Naive lymphocytes were incubated with nano-aAPC bearing Db-GP100, Kb-SIINF, and Kb-TRP2, each at the standard single-antigen dose. One week after "triple" E+E, antigen-specific T cells were detected by pentamer staining against each antigen of interest (Figure 3F). While the frequency of each population was lower than that found with T-cells stimulated with only one antigen (Figure 3G), the total number of antigen-specific T-cells was similar whether stimulated with individual antigens or with three antigens ($p > 0.4$ by two-way ANOVA) (Figure 3G). Thus, the total number of cells generated against antigens of interest was larger than for single-specificity cultures.

**Expansion of Neo-Antigens.** The tumor antigens described thus far are previously known "shared antigens" derived from proteins that are overexpressed in tumors, and present on or shared between tumors from multiple patients. With the advent of genome-wide sequencing, it has been shown that most cancers contain clonal, nonsynonymous single base pair substitutions that may bind to the patient's MHC, thereby opening up new avenues for immunotherapy.[29] Subsequent analyses have reinforced this idea.[38−45] These "neo-antigens" have theoretical advantages over shared antigens as tumor targets, such as greater specificity for tumor tissue and potentially higher-affinity TCR-MHC interactions. However, the pattern of mutation is unique in each cancer, and methods must be developed for rapid personalized identification and targeting of these neo-antigens.

To generate T cell responses against neo-antigens using Enrichment + Expansion, we utilized published "mutomes" described for the mouse melanoma line B16 and colon carcinoma line CT26.[46,47] Briefly, genomic and transciptomic data sets were combined to identify expressed single base pair substitutions (Figure 4A). Eight or nine flanking amino acids upstream and downstream of each SBS were extracted *in silico*. These ∼17-amino acid sequences were then processed by NetMHC, an algorithm that predicts binding of peptides to human HLA as well as mouse MHC alleles using an artificial neural network.[48] This algorithm predicted amino acid neo-epitopes 8 to 10 amino acids in length for CT26 and B16 (Table S2). Seven candidate peptides representing a wide range of predicted affinities, 2 from CT26 and 5 from B16, were synthesized and used to generate neo-epitope specific nano-aAPC. E+E with nano-aAPC bearing these neo-epitopes was then performed and evaluated with MHC multimers at Day 7.

Antigen-specific populations from Day 7 cultures were identified for both of the two CT26-derived candidate peptides tested (FPS and SAF). Figure 4B shows representative Day 7 cognate MHC staining of Ld-FPS and Ld-SAF activated samples. Peptides derived from the B16 mutome showed responsive (Db-YTG) and nonresponsive (Kb-LAY) staining patterns (Figure 4B); overall 2/5 peptides explored (Db-YTG and Kb-VDW) showed strong responses, 2/5 showed moderate responses (Db-IAM and Db-RTF), and 1/5 was nonresponsive (Kb-LAY). Peptide affinity for MHC as predicted by NetMHC (Table S2) did not accurately predict E+E response; strong responders YTG and VDW had low predicted affinities at 991 and 9066 nM respectively, whereas the nonresponder LAY and equivocal responder IAM had high predicted affinities at 69 and 5 nM respectively. Overall, the total

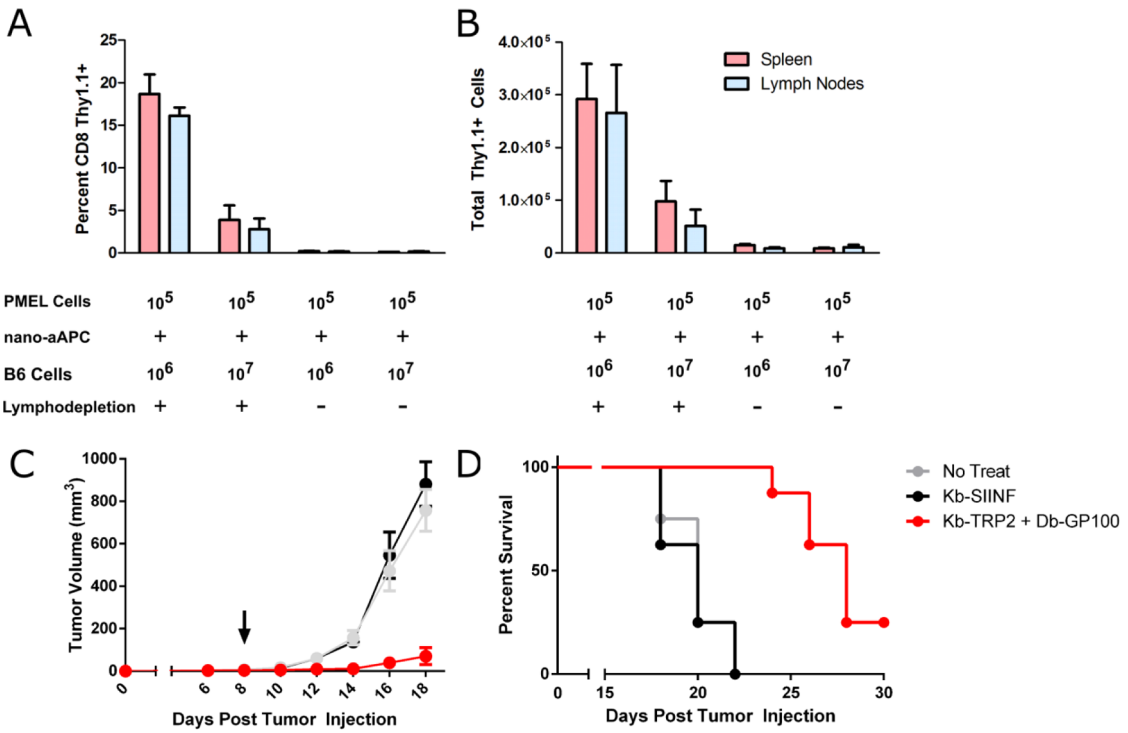


**Figure 5. Adoptive transfer of E+E T cells mediates tumor rejection. (A) Effect of lymphodepletion and decreased bystander competition on expansion after adoptive transfer. B6 mice were untreated or lymphodepleted with 500 cGy $\gamma$ radiation 1 day prior to adoptive transfer of $10^5$ previously activated pmel T cells in the presence of either $10^6$ or $10^7$ irrelevant B6 cells. Both lymphodepletion and administration of fewer bystander cells increased the frequency of pmel T cells recovered from spleen (pink) and lymph nodes (blue) ($p < 0.01$ by two-way ANOVA). (B) Total number of Thy1.1+ pmel cells recovered in A. (C) Kb-TRP2 and Db-GP100 Enriched + Expanded lymphocytes cultured for 7 days prior to adoptive transfer inhibited melanoma growth ($p < 0.01$ by two-way ANOVA, 8 mice/group, red). Mice were injected with subcutaneous melanoma 8 days prior and irradiated with 500 cGy gamma irradiation 1 day prior. Noncognate E+E lymphocytes (SIINF; black) did not inhibit tumor growth (compared to untreated, gray), whereas cognate E+E (TRP2+GP100, red) did. (D) Survival of animals from C. 2/8 mice showed complete rejection of tumors in the Kb-TRP2 and Db-GP100 treated group, which had significantly longer survival compared to noncognate and untreated groups ($p < 0.01$ by Mantel-Cox).**

number of cells generated at Day 7 approximated those observed with the shared antigens Db-GP100 and Ld-A5, ranging from 15 000−40 000 (Figure 4C), but was less than the shared antigens Kb-TRP2 and Kb-SIIN.

**Effect of Enrichment on Proliferation After Adoptive Transfer.** The use of enrichment in addition to expansion is motivated by the observation that adoptively transferred tumor-specific T cells compete with cotransferred, nontumor specific T-cells for growth signals.[49−51] However, this effect has not been demonstrated for antigen-specific T cells that have been previously activated *in vitro*, as occurs during E+E. We thus combined tumor-specific pmel T cells and polyclonal, wild-type B6 T cells in ratios that approximated the antigen specific frequencies achieved with and without E+E (10% and 1%, respectively). In each group, the total number of pmel T cells administered was the same ($10^5$); only the amount of nonspecific T cells differed ($10^6$ or $10^7$). The largest number and highest frequency of pmel T cells were observed in mice receiving fewer ($10^6$) nonspecific T-cells (Figure 5A,B). Approximately $5.5 \pm 1.5 \times 10^5$ pmel T cells were recovered from the spleen and lymph nodes of these animals (Figure 5B). Only $1.4 \pm 0.7 \times 10^5$ pmel T cells were recovered from animals receiving $10^7$ nonspecific T-cells ($p < 0.05$ by two-way ANOVA with Tukey post-test). Thus, removal of competition from cotransferred cells enhanced engraftment and expansion after transfer.

In addition, tumor-specific T cells compete with *host* cells for growth signals,[52] which has motivated the use of host radio- and chemo-based lymphodepletion prior to adoptive transfer.[53,54] Thus, animals receiving $10^6$ or $10^7$ nonspecific T-cells were either irradiated with 500 cGy $\gamma$ radiation 24 h prior to transfer or left untreated, generating four experimental groups. Animals that were not irradiated showed poor engraftment, with less than $0.3 \times 10^5$ pmel T cells recovered in either the $10^6$ or $10^7$ bystander group (Figure 5A,B). Thus, removal of both transferred bystander lymphocytes and host lymphocytes significantly increased the yield of adoptively transferred tumor-specific T cells in the host.

**Tumor Killing Using Enriched and Expanded T cells.** We next determined whether tumor-specific lymphocytes generated by E+E could mediate rejection of established melanoma. B16−F10 cells, which form aggressive and poorly immunogenic melanomas, were implanted

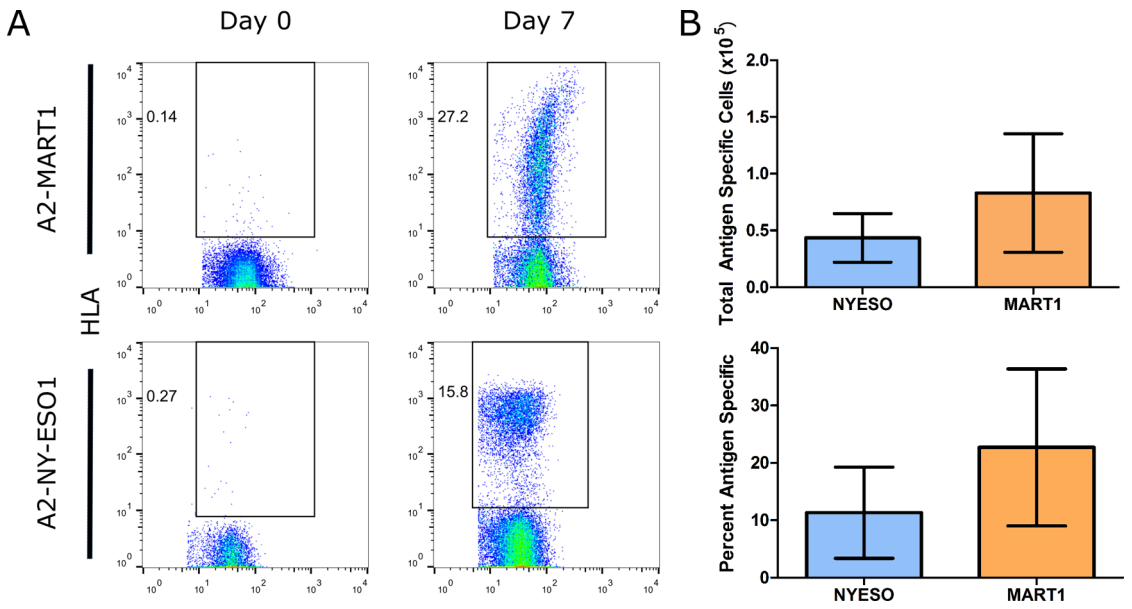


**Figure 6. Expansion of human antitumor response. CD8+ PBMCs were isolated from healthy donors and expanded using E+E for 1 week. (A) Representative staining and frequency of A2-NY-ESO1 (top) and A2-MART1 (bottom) specific cells immediately after CD8 isolation (Day 0, left) and after 1 week of E+E (Day 7, right). (B) Summary of total antigen-specific cells (top) and percent antigen-specific cell frequency (bottom) after E+E with indicated nano-aAPC. Results derived from three experiments with different donors.**

subcutaneously into B6 host mice and allowed to grow for 8 days until tumors were palpable. In parallel, CD8 lymphocytes were isolated from naive B6 donor mice and Enriched + Expanded against Db-GP100 and Kb-TRP2 antigens for 7 days, then transferred into hosts 1 day after lymphodepletion.

Animals receiving tumor-specific E+E donor lymphocytes had significantly less tumor growth than untreated mice or mice receiving equivalent numbers of lymphocytes generated against irrelevant Kb-SIINF antigen (Figure 5C). Eighteen days after tumor injection, mean tumor volume in untreated mice was 757 ± 98 $mm^3$, similar to Kb-SIINF treated mice (881 ± 104 $mm^3$) but much greater than in Db-GP100/Kb-TRP2 treated mice (70 ± 40 $mm^3$; $p < 0.05$ by ANOVA with Tukey post-test).

All mice in untreated and Kb-SIINF treated groups were sacrificed by day 22 due to excessive tumor burden. By comparison, no mice in the Db-GP100/Kb-TRP2 group were sacrificed until day 24, and 2/8 mice had no detectable tumor 2 months after implantation ($p < 0.01$ by Mantel-Cox). Median survival was significantly greater in the E+E treated group (28 days) than the untreated (20 days) or noncognate treated (20 days) group. Thus, E+E lymphocytes cultured from naive cells for only a week were able to delay and in some cases completely reject established B16 melanoma.

**Expansion of Human Tumor Antigens.** Enrichment + Expansion with nano-aAPC functionalized with human HLA-A2 permitted robust expansion against the tumor antigens NY-ESO-1 and MART1 from naïve donors. Human CD8+ lymphocytes were isolated from peripheral blood mononuclear cells of healthy donors, and E+E was performed with nano-aAPC bearing either NY-ESO1 or MART1 tumor antigens. After 1 week, 44 000 ± 21 000 NY-ESO1 specific cells were generated, representing approximately 1000-fold precursor expansion (Table 1, Figure 6). For MART1 responses, 83 000 ± 37 000 were generated in 1 week; this represents approximately 100-fold expansion, reflecting the high precursor frequency of MART1 responses found even in healthy donors[55] (Table 1, Figure 6). Expansion was significantly enhanced by coupling MHC to a solid aAPC support, as soluble MHC-peptide did not induce significant expansion (Figure S5a). Thus, Enrichment + Expansion is not limited to murine T cells, but is also a robust approach for the expansion of naïve, low frequency, antitumor human CTL.

## CONCLUSION

Widespread application of adoptive immunotherapy for cancer is limited by the availability of safe, cost-effective and convenient sources of tumor-specific cells. Here, we developed a streamlined technology for quickly expanding large numbers of high frequency tumor-specific lymphocytes from naive cells, with more than 1000-fold expansion in 1 week. Removing irrelevant cells by enrichment confers a 3−10 fold increase in total antigen-specific cell number after *in vitro* culture, and a 3−4 fold increase after *in vivo* transfer, resulting in approximately 10−40 fold increase in total antigen-specific cells in the host.

While antigen-specific T cells can be enriched using MHC tetramers after T cell expansion,[56−58] our

platform simplifies this process by coupling enrichment and expansion in a single reagent. Furthermore, cross-linking of TCR by multimeric MHC in the absence of costimulation can induce T cell apoptosis or anergy,[59−61] with deletion of up to one-half of antigen-specific cells after tetramer engagement.

Furthermore, we have previously reported on the use of magnetic fields as a method to induce clustering of paramagnetic-particle bound TCR, enhancing T cell activation.[17] Nano-aAPC bound to T cells in a magnetic field aggregate on the cell surface, inducing CD3 clustering, strong T cell activation and up to 5-fold increased expansion. The contribution of magnet-induced clustering during E+E remains to be explored, but may represent an additional method for enhancing T cell activation during magnetic enrichment with nanoparticles.

E+E compared favorably, both in terms of total number and purity, to existing attempts to generate robust expansion in a short period. For example, expansion of NY-ESO1 specific T cells with dendritic cell-based methods after 1 week in culture is either undetectable or not reported (Table S3), making the achievement of antigen specific purities between 4 and 27% with 1000-fold expansion all the more remarkable. In contrast, several groups have reported effective expansion of the high precursor frequency MART1 response (Table S3). For example, the DC-based ACE-CD8 platform described by Wölfl *et al.*[62] is a well-characterized system that has been useful for defining and optimizing requirements for expansion of human CD8 cells. This procedure results in an impressive 10 day expansion; however, the lack of a cellular expansion platform or feeder cell remains a primary advantage of nano-aAPC based approaches, eliminating the need for additional plasmapharesis or culture to generate activator cells.

Assuming tumor-specific T cell precursor frequencies of approximately 1−10 per million, $\sim 0.5 \times 10^{10}$ CD8 T cells harvested from a single leukapharesis, and 1000−5000 fold expansion with E+E, more than $10^8$ antigen specific T cells could be generated in 1 week, possibly sufficient for therapy.[63−65] We were further able to simultaneously expand T cell responses against three antigens in a single culture without loss of total cell yield for any single antigen; this suggests that proliferation under these conditions is limited by T cell proliferative response rather than culture media or cytokine support, and that simultaneously expanding multiple antigens would increase the total tumor cell yield, generating sufficient cells for infusion ($10^8$ to $10^{10}$ tumor-reactive T cells[63−65]).

We also generated antigen-specific responses to predicted neo-epitopes, with response sizes on the order of magnitude seen with shared tumor antigens. Our success rate, 6/7, was higher than that described in previously published reports,[46] likely reflecting use of an experimentally curated mutome that may not be representative of candidate lists obtained using current prediction algorithms. Nevertheless, our approach represents a proof-of-concept method for rapid expansion and validation of neo-epitopes for specific immunotherapy based on computational prediction and expansion with E+E.

Tumor-specific neo-epitopes can be identified across a wide variety of cancers,[39] with certain stereotypical mutations in oncogene hotspots such as codons 12, 13, and 61 of *kras* shared in up to 30% of patients,[40] in addition to a large number of patient-specific mutations. This suggests two possible therapeutic strategies: (1) a *precision* approach, where a small number of commonly shared neo-epitopes are expanded using off-the-shelf nano-aAPC, and (2) a fully *personalized* approach, where custom-tailored aAPC are designed after whole-exome sequencing and neo-epitope prediction. The optimal strategy will likely depend on a patient's unique mutation burden, as well as the frequency of tumor-specific responses that can be generated in a given individual. This latter parameter remains poorly characterized, and we propose that Enrichment + Expansion could serve as a rapid assay for characterizing the tumor-specific T cell repertoire.

In summary, by eliminating the need to culture cellular APCs and streamlining the generation of large numbers of high-frequency tumor-specific T cells, Enrichment + Expansion improves upon existing methods for T cell expansion from naïve precursors, and may be a powerful addition to autologous tumor immunotherapy protocols.

## MATERIALS AND METHODS

**Mice and Reagents.** Pmel TCR/Thy1$^a$ Rag−/− transgenic mice were a gift from Nicholas Restifo (National Institutes of Health, Bethesda, MD) and maintained as homozygotes. C57BL/6j and Balb/C mice were purchased from Jackson Laboratories (Bar Harbor, ME). All mice were maintained according to Johns Hopkins University's Institutional Review Board. Fluorescently labeled monoclonal antibodies were purchased from BioLegend (San Diego, CA) and BD (San Jose, CA).

**Preparation of MHC-Ig Dimers and Nano-aAPC.** Soluble MHC-Ig dimers, $K^b$-Ig, $D^b$-Ig, and A2-Ig were prepared and loaded with peptides as described,[34] see Supporting Information Methods. Nano-aAPC were manufactured by direct conjugation of MHC-Ig dimer and anti-CD28 antibody (37.51; BioLegend) to MACS Microbeads (Miltenyi Biotec) as described previously[14] or by conjugating biotinylated signal 1 and signal 2 to anti-biotin beads (Miltenyi Biotec).

**Lymphocyte Isolation.** Mouse lymphocytes were obtained from homogenized mouse spleens and lymph nodes after hypotonic lysis of RBC. Cytotoxic lymphocytes were isolated using a CD8 magnetic enrichment column from Miltenyi Biotec (Cologne, Germany) following the manufacturer's instructions.

When applicable, cells were labeled with carboxyfluorescein succinimidyl ester (CFSE) for 15 min at 37 °C, then washed extensively. For human studies, the ethical committee of the Johns Hopkins University approved this study and all healthy volunteers gave written informed consent. PBMC of HLA-A2$^+$ donors were obtained by density gradient centrifugation (Lymphocyte Separation Medium Ficoll-Paque, GE Healthcare). Subsequently, CD8$^+$ T cells were isolated using a CD8 magnetic enrichment column from Miltenyi Biotec (Cologne, Germany).

**Enrichment and Expansion.** Nano-aAPC were stored at a concentration of 8.3 nM ($5 \times 10^{12}$ particles/mL), and all volumes refer to particles at this concentration. Ten million CD8-enriched lymphocytes at $\sim 10^8$ cells/mL were incubated with 10 $\mu$L of nano-aAPC for 1 h at 4 °C, for an approximate bead:cell concentration of 5000:1. Cell-particle mixtures were subsequently passed through a magnetic enrichment column, the negative fraction was collected and the positive fraction eluted. Isolated fractions were mixed and cultured in 96-well round-bottom plates for 7 days in complete RPMI-1640 medium supplemented with 10% human autologous serum and 3% T cell growth factor, a cytokine cocktail derived from stimulated PBMC as described in the literature,[66] in a humidified 5% $CO_2$, 37 °C incubator for 1 week. Specificity of CTL was monitored on day 0 and 7, by FACS analysis following tetramer and dimeric MHC-Ig staining. The number of antigen-specific cells was calculated by multiplying the number of total cells by the fractions of CD8 and antigen-specific cells; the fraction of antigen-specific cells was calculated after subtracting the non-cognate MHC staining from cognate MHC staining.

**Neo-Epitope Prediction.** The DNA and RNA from CT26 cells were used to identify somatic mutations and the transcriptome of this line through massively parallel sequencing. The methods used to prepare libraries for analysis on an Illumina HiSeq 2500 instrument are described in [47]. The predictions of neo-epitopes were performed as previously described, with the exception that netMHCpan was used for epitope prediction.[47] Briefly, genomic and transciptomic data sets were combined to identify expressed single base pair substitutions (SBS). The eight flanking amino acids upstream and downstream of each SBS were extracted *in silico*. This 17-amino acid peptide sequence was then processed by NetMHCpan version 2.4 to identify moderate (<500 nM) to high (<50 nM) affinity 9-amino acid peptides for all H-2d alleles. Candidate epitopes were then selected from among these moderate to high affinity peptides for experimental testing.

The B16 murine melanoma line was previously sequenced and 50 expressed mutations identified.[46] In that paper, mutations were tested for their ability to elicit an immune response relative to the wild type peptide; however, detailed peptide epitopes were not identified. Full protein sequences were determined from Uniprot.org, from which nine flanking amino acids upstream and downstream of each mutation were extracted. Each 19-amino acid sequence was processed by NetMHC versions 3.4 and 3.2 to determine H-2b binding affinity of potential 8-, 9-, and 10-amino acid binders. For each SBS, the highest affinity peptide was selected for further analysis. A list of top candidate epitopes was compiled based on the epitope meeting either of the following criteria: (1) moderate to high affinity predicted binding affinity to H-2b allele, or (2) higher mutant peptide immunogenicity relative to the wild type peptide, based on the work of Castle *et al.*

**Bystander *In Vivo* Experiments.** Mixtures of pmel and wild-type B6 CD8+ T lymphocytes were mixed at the indicated ratios. Cell mixtures were cultured for 1 week with 20 $\mu$L of Db-GP100 nano-aAPC prior to adoptive transfer to activate PMEL T cells. Transient lymphopenia was induced in host mice by sublethal irradiation (500 cGy) 1 day before adoptive transfer with a MSD Nordion Gammacell dual Cs137 source (Johns Hopkins Molecular Imaging Center) in the indicated groups. Mice were treated both the day of and the day after adoptive transfer with 30 000 units intraperitoneal IL-2. Seven and twenty-days after adoptive transfer, three mice per group were sacrificed and lymphocytes were isolated from peripheral blood, spleen, and inguinal, cervical, and axillary lymph nodes, and then stained with anti-Thy1.1 antibody.

**Therapeutic T Cell Transfer.** Tumor rejection experiments were performed as described above, except $3 \times 10^5$ B16 melanoma cells were injected subcutaneously 10 days prior to adoptive T cell transfer. Transient lymphopenia was induced 1 day before adoptive transfer sublethal irradiation. Ten million naive lymphocytes from each donor were used to generate antigen-specific cells for each tumor-bearing host (up to 3 hosts per donor), containing approximately $2 \times 10^5$ tumor-specific T cells per mouse. Mice were treated with 30 000 units intraperitoneal IL-2 1 day before and 1 day after adoptive transfer of T-cells. Tumor growth was monitored at 2-day intervals using digital calipers, with volume calculated using an ellipsoid approximate, volume = 1/2 × length × width. Mice were sacrificed once tumors reached 900 mm$^3$.

*Conflict of Interest:* The authors declare the following competing financial interest(s): Under a licensing agreement between NexImmune and the Johns Hopkins University, JPS and MO are entitled to a share of royalty received by the University on sales of products derived from this article. The terms of this arrangement are being managed by the Johns Hopkins University in accordance with its conflict of interest policies.

*Acknowledgment.* We thank M. Niemöller, A. Richter, M. Assenmacher of Miltenyi Biotec for assistance with preparation of the nano-aAPC. Recombinant IL-2 was a gift from Prometheus Laboratories Inc., San Diego. This work was supported by the National Institutes of Health (AI072677, GM 07309, AI44129, CA 43460, CA 62924, CA 09243, and CA108835), The Troper Wojcicki Foundation, The Virginia and D.K. Ludwig Fund for Cancer Research, The Sol Goldman Center for Pancreatic Cancer Research, The Commonwealth Foundation, and a sponsored research agreements with Miltenyi Biotec and NexImmune. Antibody and lymphocyte images reproduced under a Creative Commons License from Servier Medical Art (http://www.servier.com/Powerpoint-image-bank). K. Perica is supported in part by a Cancer Research Institute Predoctoral Fellowship. C. Schütz is supported by a German Research Foundation (DFG) Postdoctoral Fellowship (SCHU-2681/1-1) and a HERA Women's Cancer Foundation OSB1 Grant. KP, MO, and JPS conceived of nano-aAPC for T cell activation. KP, JGB and JPS conceived of enrichment and expansion with nano-aAPC. KP and JPS designed experiments and wrote the first draft of the manuscript. KP and JGB performed mouse experiments. CS, JCV, and YLC performed human lymphocytes expansion experiments. JD, AS, KWK, BV, and SZ created and tested neo-epitope predictions. All authors contributed to final writing of the manuscript.

*Supporting Information Available:* Five figures and three tables. Effect of Enrichment on Antigen Specific Frequency and Total Cells. Micro-aAPC Enrichment. Characterization of Fold-Expansion and Phenotype. T Cell Expansion with Bone-Marrow Derived DCs. Comparison to Existing Technologies. Candidate Neo-Epitopes. Representative T Cell Expansion After One Week. Expansion with Soluble MHC-Peptide. The Supporting Information is available free of charge on the ACS Publications website at DOI: 10.1021/acsnano.5b02829.

## REFERENCES AND NOTES

1. Restifo, N. P.; Dudley, M. E.; Rosenberg, S. a. Adoptive Immunotherapy for Cancer: Harnessing the T Cell Response. *Nat. Rev. Immunol.* **2012**, *12*, 269–281.
2. Barrett, D. M.; Singh, N.; Porter, D. L.; Grupp, S. a; June, C. H. Chimeric Antigen Receptor Therapy for Cancer. *Annu. Rev. Med.* **2014**, *65*, 333–347.
3. Kershaw, M. H.; Westwood, J. a; Darcy, P. K. Gene-Engineered T Cells for Cancer Therapy. *Nat. Rev. Cancer* **2013**, *13*, 525–541.
4. Yee, C. The Use of Endogenous T Cells for Adoptive Transfer. *Immunol. Rev.* **2014**, *257*, 250–263.
5. Morgan, R. A.; Chinnasamy, N.; Abate-daga, D.; Gros, A.; Robbins, P. F.; Zheng, Z.; Dudley, M. E.; Feldman, S. A.; Yang, J. C.; Sherry, R. M.; *et al.* Cancer Regression and Neurological Toxicity Following Anti-Mage-A3 TCR Gene Therapy. *J. Immunother.* **2013**, *36*, 133–151.

6. Zhong, S.; Malecek, K. T-Cell Receptor Affinity and Avidity Defines Antitumor Response and Autoimmunity in T-Cell Immunotherapy. *Proc. Natl. Acad. Sci. U. S. A.* **2013**, DOI: 10.1073/pnas.1221609110.
7. Wherry, E. J. T Cell Exhaustion. *Nat. Immunol.* **2011**, *131*, 492–499.
8. Rabinovich, G. a; Gabrilovich, D.; Sotomayor, E. M. Immunosuppressive Strategies That Are Mediated by Tumor Cells. *Annu. Rev. Immunol.* **2007**, *25*, 267–296.
9. Dudley, M. E.; Rosenberg, S. a. Adoptive-Cell-Transfer Therapy for the Treatment of Patients with Cancer. *Nat. Rev. Cancer* **2003**, *3*, 666–675.
10. Itzhaki, O.; Hovav, E.; Ziporen, Y.; Levy, D.; Kubi, A.; Zikich, D.; Hershkovitz, L.; Treves, A. J.; Shalmon, B.; Zippel, D.; *et al.* Establishment and Large-Scale Expansion of Minimally Adoptive Transfer Therapy. *J. Immunother.* **2011**, *34*, 212–220.
11. Satthaporn, S.; Robins, A.; Vassanasiri, W.; El-Sheemy, M.; Jibril, J. a; Clark, D.; Valerio, D.; Eremin, O. Dendritic Cells Are Dysfunctional in Patients with Operable Breast Cancer. *Cancer Immunol. Immunother.* **2004**, *53*, 510–518.
12. Hurwitz, A. a; Watkins, S. K. Immune Suppression in the Tumor Microenvironment: A Role for Dendritic Cell-Mediated Tolerization of T Cells. *Cancer Immunol. Immunother.* **2012**, *61*, 289–293.
13. Ma, Y.; Shurin, G. V.; Gutkin, D. W.; Shurin, M. R. Tumor Associated Regulatory Dendritic Cells. *Semin. Cancer Biol.* **2012**, *22*, 298–306.
14. Perica, K.; De León Medero, A.; Durai, M.; Chiu, Y. L.; Bieler, J. G.; Sibener, L.; Niemöller, M.; Assenmacher, M.; Richter, A.; Edidin, M.; *et al.* Nanoscale Artificial Antigen Presenting Cells for T Cell Immunotherapy. *Nanomedicine* **2013**, *10*, 119–129.
15. Zhang, N.; Bevan, M. J. CD8(+) T Cells: Foot Soldiers of the Immune System. *Immunity* **2011**, *35*, 161–168.
16. Fahmy, T. M.; Bieler, J. G.; Edidin, M.; Schneck, J. P. Increased TCR Avidity after T Cell Activation: A Mechanism for Sensing Low-Density Antigen. *Immunity* **2001**, *14*, 135–143.
17. Perica, K.; Tu, A.; Richter, A.; Bieler, J. G.; Edidin, M.; Schneck, J. P. Magnetic Field-Induced T Cell Receptor Clustering by Nanoparticles Enhances T Cell Activation and Stimulates Antitumor Activity. *ACS Nano* **2014**, *8*, 2252–2260.
18. He, C.; Hu, Y.; Yin, L.; Tang, C.; Yin, C. Effects of Particle Size and Surface Charge on Cellular Uptake and Biodistribution of Polymeric Nanoparticles. *Biomaterials* **2010**, *31*, 3657–3666.
19. Decuzzi, P.; Godin, B.; Tanaka, T.; Lee, S.-Y.; Chiappini, C.; Liu, X.; Ferrari, M. Size and Shape Effects in the Biodistribution of Intravascularly Injected Particles. *J. Controlled Release* **2010**, *141*, 320–327.
20. Semete, B.; Booysen, L.; Lemmer, Y.; Kalombo, L.; Katata, L.; Verschoor, J.; Swai, H. S. In Vivo Evaluation of the Biodistribution and Safety of PLGA Nanoparticles as Drug Delivery Systems. *Nanomedicine* **2010**, *6*, 662–671.
21. Schamel, W. W. a; Alarcón, B. Organization of the Resting TCR in Nanoscale Oligomers. *Immunol. Rev.* **2013**, *251*, 13–20.
22. Rizzuto, G. a; Merghoub, T.; Hirschhorn-Cymerman, D.; Liu, C.; Lesokhin, A. M.; Sahawneh, D.; Zhong, H.; Panageas, K. S.; Perales, M.-A.; Altan-Bonnet, G.; *et al.* Self-Antigen-Specific CD8+ T Cell Precursor Frequency Determines the Quality of the Antitumor Immune Response. *J. Exp. Med.* **2009**, *206*, 849–866.
23. Jenkins, M. K.; Chu, H. H.; McLachlan, J. B.; Moon, J. J. On the Composition of the Preimmune Repertoire of T Cells Specific for Peptide-Major Histocompatibility Complex Ligands. *Annu. Rev. Immunol.* **2010**, *28*, 275–294.
24. Jenkins, M. K.; Moon, J. J. The Role of Naive T Cell Precursor Frequency and Recruitment in Dictating Immune Response Magnitude. *J. Immunol.* **2012**, *188*, 4135–4140.
25. Chapuis, A.; Ragnarsson, G. Transferred WT1-Reactive CD8+ T Cells Can Mediate Antileukemic Activity and Persist in Post-Transplant Patients. *Sci. Transl. Med.* **2013**, *5*, 174ra27.
26. Klebanoff, C. a; Gattinoni, L.; Palmer, D. C.; Muranski, P.; Ji, Y.; Hinrichs, C. S.; Borman, Z. a; Kerkar, S. P.; Scott, C. D.; Finkelstein, S. E.; *et al.* Determinants of Successful CD8+ T-Cell Adoptive Immunotherapy for Large Established Tumors in Mice. *Clin. Cancer Res.* **2011**, *17*, 5343–5352.
27. Wen, F.; Thisted, R. A Systematic Analysis of Experimental Immunotherapies on Tumors Differing in Size and Duration of Growth. *Oncoimmunology* **2012**, 172–178.
28. Besser, M. J.; Shapira-Frommer, R.; Treves, A. J.; Zippel, D.; Itzhaki, O.; Hershkovitz, L.; Levy, D.; Kubi, A.; Hovav, E.; Chermoshniuk, N.; *et al.* Clinical Responses in a Phase II Study Using Adoptive Transfer of Short-Term Cultured Tumor Infiltration Lymphocytes in Metastatic Melanoma Patients. *Clin. Cancer Res.* **2010**, *16*, 2646–2655.
29. Segal, N. H.; Parsons, D. W.; Peggs, K. S.; Velculescu, V.; Kinzler, K. W.; Vogelstein, B.; Allison, J. P. Epitope Landscape in Breast and Colorectal Cancer. *Cancer Res.* **2008**, *68*, 889–892.
30. Smith-Garvin, J. E.; Koretzky, G. a; Jordan, M. S. T Cell Activation. *Annu. Rev. Immunol.* **2009**, *27*, 591–619.
31. Durai, M.; Krueger, C.; Ye, Z.; Cheng, L.; Mackensen, A.; Oelke, M.; Schneck, J. P. In Vivo Functional Efficacy of Tumor-Specific T Cells Expanded Using HLA-Ig Based Artificial Antigen Presenting Cells (aAPC). *Cancer Immunol. Immunother.* **2009**, *58*, 209–220.
32. Sarkar, S.; Teichgräber, V.; Kalia, V.; Polley, A.; Masopust, D.; Harrington, L. E.; Ahmed, R.; Wherry, E. J. Strength of Stimulus and Clonal Competition Impact the Rate of Memory CD8 T Cell Differentiation. *J. Immunol.* **2007**, *179*, 6704–6714.
33. Oelke, M.; Kurokawa, T.; Hentrich, I.; Behringer, D.; Cerundolo, V.; Lindemann, A. Functional Characterization of CD8 1 Antigen-Specific Cytotoxic T Lymphocytes after Enrichment Based on Cytokine Secretion: Comparison with the MHC-Tetramer Technology. *Scand. J. Immunol.* **2000**, 544–549.
34. Oelke, M.; Maus, M. V.; Didiano, D.; June, C. H.; Mackensen, A.; Schneck, J. P. Ex Vivo Induction and Expansion of Antigen-Specific Cytotoxic T Cells by HLA-Ig-Coated Artificial Antigen-Presenting Cells. *Nat. Med.* **2003**, *9*, 619–624.
35. Seliger, B. Molecular Mechanisms of MHC Class I Abnormalities and APM Components in Human Tumors. *Cancer Immunol. Immunother.* **2008**, *57*, 1719–1726.
36. Kaluza, K. M.; Thompson, J. M.; Kottke, T. J.; Flynn Gilmer, H. C.; Knutson, D. L.; Vile, R. G. Adoptive T Cell Therapy Promotes the Emergence of Genomically Altered Tumor Escape Variants. *Int. J. Cancer* **2012**, *131*, 844–854.
37. Jensen, S. M.; Twitty, C. G.; Maston, L. D.; Antony, P. a; Lim, M.; Hu, H.-M.; Petrausch, U.; Restifo, N. P.; Fox, B. a. Increased Frequency of Suppressive Regulatory T Cells and T Cell-Mediated Antigen Loss Results in Murine Melanoma Recurrence. *J. Immunol.* **2012**, *189*, 767–776.
38. Duan, F.; Duitama, J.; Al Seesi, S.; Ayres, C. M.; Corcelli, S. a.; Pawashe, a. P.; Blanchard, T.; McMahon, D.; Sidney, J.; Sette, a.; *et al.* Genomic and Bioinformatic Profiling of Mutational Neoepitopes Reveals New Rules to Predict Anticancer Immunogenicity. *J. Exp. Med.* **2014**, *211*, 2231.
39. Rajasagi, M.; Shukla, S. a; Fritsch, E. F.; Keskin, D. B.; DeLuca, D.; Carmona, E.; Zhang, W.; Sougnez, C.; Cibulskis, K.; Sidney, J.; *et al.* Systematic Identification of Personal Tumor-Specific Neoantigens in Chronic Lymphocytic Leukemia. *Blood* **2014**, *124*, 453–462.
40. Fritsch, E. F.; Rajasagi, M.; Ott, P. a; Brusic, V.; Hacohen, N.; Wu, C. J. HLA-Binding Properties of Tumor Neoepitopes in Humans. *Cancer Immunol. Res.* **2014**, *2*, 522–529.
41. Srivastava, P. K.; Duan, F. Harnessing the Antigenic Fingerprint of Each Individual Cancer for Immunotherapy of Human Cancer: Genomics Shows a New Way and Its Challenges. *Cancer Immunol. Immunother.* **2013**, *62*, 967–974.
42. Tran, E.; Turcotte, S.; Gros, A.; Robbins, P. F.; Lu, Y.; Dudley, M. E.; Parkhurst, M. R.; Yang, J. C.; Rosenberg, S. A. Cancer Immunotherapy Based on Mutation-Specific CD4+ T Cells in a Patient with Epithelial Cancer. *Science* **2014**, *344*, 641–645.

43. Matsushita, H.; Vesely, M.; Koboldt, D. Cancer Exome Analysis Reveals a T-Cell-Dependent Mechanism of Cancer Immunoediting. *Nature* **2012**, *482*, 400–404.
44. Yadav, M.; Jhunjhunwala, S.; Phung, Q. T.; Lupardus, P.; Tanguay, J.; Bumbaca, S.; Franci, C.; Cheung, T. K.; Fritsche, J.; Weinschenk, T.; *et al.* Predicting Immunogenic Tumour Mutations by Combining Mass Spectrometry and Exome Sequencing. *Nature* **2014**, *515*, 572–576.
45. Gubin, M. M.; Zhang, X.; Schuster, H.; Caron, E.; Ward, J. P.; Noguchi, T.; Ivanova, Y.; Hundal, J.; Arthur, C. D.; Krebber, W.-J.; *et al.* Checkpoint Blockade Cancer Immunotherapy Targets Tumour-Specific Mutant Antigens. *Nature* **2014**, *515*, 577–581.
46. Castle, J. C.; Kreiter, S.; Diekmann, J.; Löwer, M.; van de Roemer, N.; de Graaf, J.; Selmi, A.; Diken, M.; Boegel, S.; Paret, C.; *et al.* Exploiting the Mutanome for Tumor Vaccination. *Cancer Res.* **2012**, *72*, 1081–1091.
47. Kim, K.; Skora, A. D.; Li, Z.; Liu, Q.; Tam, A. J.; Blosser, R. L.; Diaz, L. a; Papadopoulos, N.; Kinzler, K. W.; Vogelstein, B.; *et al.* Eradication of Metastatic Mouse Cancers Resistant to Immune Checkpoint Blockade by Suppression of Myeloid-Derived Cells. *Proc. Natl. Acad. Sci. U. S. A.* **2014**, *111*, 11774–11779.
48. Gulukota, K.; Sidney, J.; Sette, a; DeLisi, C. Two Complementary Methods for Predicting Peptides Binding Major Histocompatibility Complex Molecules. *J. Mol. Biol.* **1997**, *267*, 1258–1267.
49. Ernst, B.; Lee, D.; Chang, J. M.; Sprent, J.; Surh, C. D.; Cd, I. Peptide Ligands Mediating Positive Selection in the Thymus Control T Cell Survival and Homeostatic Proliferation in the Periphery. *Immunity* **1999**, *11*, 173–181.
50. Dummer, W.; Ernst, B.; Leroy, E.; Surh, C. D.; Lee, D. Autologous Regulation of Naive T Cell Homeostasis Within the T Cell Compartment. *J. Immunol.* **2001**, *166*, 2460–2468.
51. Wu, Z.; Bensinger, S. J.; Zhang, J.; Chen, C.; Yuan, X.; Huang, X.; Markmann, J. F.; Kassaee, A.; Rosengard, B. R.; Hancock, W. W.; *et al.* Homeostatic Proliferation Is a Barrier to Transplantation Tolerance. *Nat. Med.* **2004**, *10*, 87–92.
52. Klebanoff, C. a; Khong, H. T.; Antony, P. a; Palmer, D. C.; Restifo, N. P. Sinks, Suppressors and Antigen Presenters: How Lymphodepletion Enhances T Cell-Mediated Tumor Immunotherapy. *Trends Immunol.* **2005**, *26*, 111–117.
53. Wrzesinski, C.; Paulos, C. M.; Kaiser, A.; Muranski, P.; Palmer, D. C.; Gattinoni, L.; Yu, Z.; Rosenberg, S. a; Restifo, N. P. Increased Intensity Lymphodepletion Enhances Tumor Treatment Efficacy of Adoptively Transferred Tumor-Specific T Cells. *J. Immunother.* **2010**, *33*, 1–7.
54. Gattinoni, L.; Finkelstein, S. E.; Klebanoff, C. a; Antony, P. a; Palmer, D. C.; Spiess, P. J.; Hwang, L. N.; Yu, Z.; Wrzesinski, C.; Heimann, D. M.; *et al.* Removal of Homeostatic Cytokine Sinks by Lymphodepletion Enhances the Efficacy of Adoptively Transferred Tumor-Specific CD8+ T Cells. *J. Exp. Med.* **2005**, *202*, 907–912.
55. Alanio, C.; Lemaitre, F.; Law, H. K. W.; Hasan, M.; Albert, M. L. Enumeration of Human Antigen-Specific Naive CD8+ T Cells Reveals Conserved Precursor Frequencies. *Blood* **2010**, *115*, 3718–3725.
56. Lu, X.; Jiang, X.; Liu, R.; Zhao, H.; Liang, Z. Adoptive Transfer of pTRP2-Specific CTLs Expanding by Bead-Based Artificial Antigen-Presenting Cells Mediates Anti-Melanoma Response. *Cancer Lett.* **2008**, *271*, 129–139.
57. Cobbold, M.; Khan, N.; Pourgheysari, B.; Tauro, S.; McDonald, D.; Osman, H.; Assenmacher, M.; Billingham, L.; Steward, C.; Crawley, C.; *et al.* Adoptive Transfer of Cytomegalovirus-Specific CTL to Stem Cell Transplant Patients after Selection by HLA-Peptide Tetramers. *J. Exp. Med.* **2005**, *202*, 379–386.
58. Yee, C.; Savage, P. a; Lee, P. P.; Davis, M. M.; Greenberg, P. D. Isolation of High Avidity Melanoma-Reactive CTL from Heterogeneous Populations Using Peptide-MHC Tetramers. *J. Immunol.* **1999**, *162*, 2227–2234.
59. Bouquié, R.; Bonnin, A.; Bernardeau, K.; Khammari, A.; Dréno, B.; Jotereau, F.; Labarrière, N.; Lang, F. A Fast and Efficient HLA Multimer-Based Sorting Procedure That Induces Little Apoptosis to Isolate Clinical Grade Human Tumor Specific T Lymphocytes. *Cancer Immunol. Immunother.* **2009**, *58*, 553–566.
60. Cebecauer, M.; Guillaume, P.; Hozák, P.; Mark, S.; Everett, H.; Schneider, P.; Luescher, I. F. Soluble MHC-Peptide Complexes Induce Rapid Death of CD8+ CTL. *J. Immunol.* **2005**, *174*, 6809–6819.
61. Guillaume, P.; Legler, D. F.; Boucheron, N.; Doucey, M.-A.; Cerottini, J.-C.; Luescher, I. F. Soluble Major Histocompatibility Complex-Peptide Octamers with Impaired CD8 Binding Selectively Induce Fas-Dependent Apoptosis. *J. Biol. Chem.* **2003**, *278*, 4500–4509.
62. Wölfl, M.; Greenberg, P. D. Antigen-Specific Activation and Cytokine-Facilitated Expansion of Naive, Human CD8+ T Cells. *Nat. Protoc.* **2014**, *9*, 950–966.
63. Mackensen, A.; Meidenbauer, N.; Vogl, S.; Laumer, M.; Berger, J.; Andreesen, R. Phase I Study of Adoptive T-Cell Therapy Using Antigen-Specific CD8+ T Cells for the Treatment of Patients with Metastatic Melanoma. *J. Clin. Oncol.* **2006**, *24*, 5060–5069.
64. Chapuis, A.; Ragnarsson, G. Transferred WT1-Reactive CD8+ T Cells Can Mediate Antileukemic Activity and Persist in Post-Transplant Patients. *Sci. Transl. Med.* **2013**, DOI: 10.1126/scitranslmed.3004916.
65. Dudley, M. E.; Wunderlich, J.; Nishimura, M. I.; Yu, D.; Yang, J. C.; Topalian, S. L.; Schwartzentruber, D. J.; Hwu, P.; Marincola, F. M.; Sherry, R.; *et al.* Adoptive Transfer of Cloned Melanoma-Reactive T Lymphocytes for the Treatment of Patients with Metastatic Melanoma. *J. Immunother.* **2001**, *24*, 363–373.
66. Oelke, M.; Moehrle, U.; Chen, J.; Behringer, D.; Cerundolo, V.; Lindemann, A.; Mackensen, A. Generation and Purification of CD8 + Melan-A-Specific Cytotoxic T Lymphocytes for Adoptive Transfer in Tumor Immunotherapy. *Clin. Cancer Res.* **2000**, 1997–2005.